PROJECT WORK IN APPLIED PHYSICS,
SECOND CYCLE, 15 CREDITS
STOCKHOLM, SWEDEN 2022

High brightness telecom band entangled photonic source

KTH Project Report

Zesheng Xu

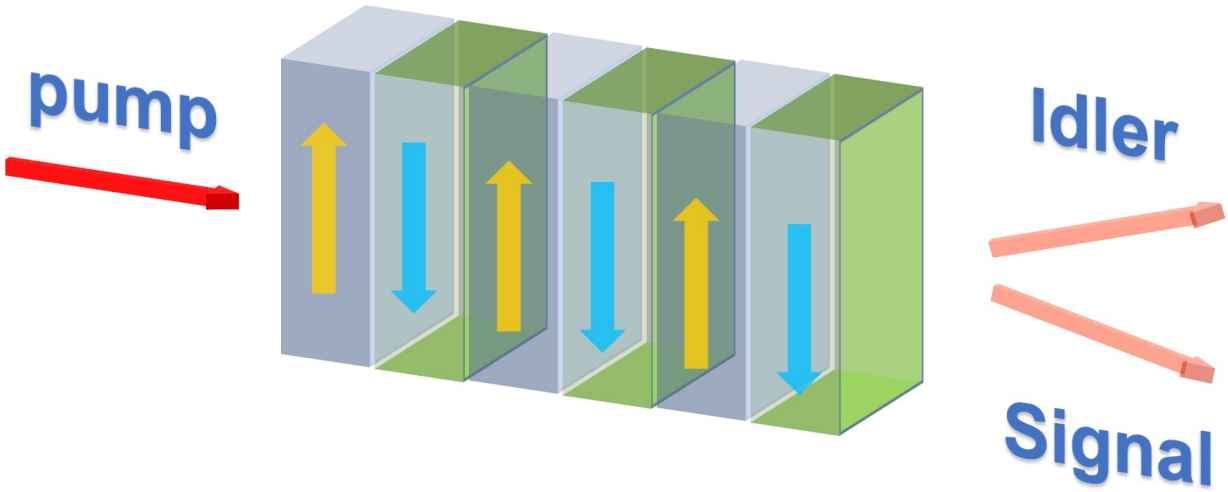

KTH ROYAL INSTITUTE OF TECHNOLOGY
Engineering Physics

Author

Zesheng Xu <zesheng@kth.se>
Applied Physics
KTH Royal Institute of Technology

Place for Project

Stockholm, Sweden
Quantum Nano photonics group-KTH

Examiner

Professor. Ulrich Vogt
KTH Royal Institute of Technology

Supervisor

Doctor. Jun Gao

Associate Professor. Ali Elshaari

KTH Royal Institute of Technology

Abstract

Quantum optical technology is a rapidly growing field which involves many sub-fields, for example, the quantum information, quantum key distribution, quantum teleportation, and quantum computation. An entangled photo-pair source with high brightness is a key to the success of many quantum optics experiments. Additionally, the telecom band is attractive for long distance communication and entanglement distribution between different nodes.

In this project, we study the theory of spontaneous parametric down-conversion (SPDC) and the property of periodically poled potassium titanyl phosphate (PPKTP). We build a high brightness entangled source with the Sagnac interferometer and test its performance.

We use high efficiency superconducting nanowire single-photon detector (SNSPD) to detect the entangled photons-paird, and we use the quTAG time tagger to collect the coincidence rate. The brightness is half million photons per second for single path and the coincidence rate is 60k per second. The visibility in $|H\rangle$ and $|+\rangle$ basis is 97.7% and 87.2%, which violates the CHSH inequality with obtained S value of 2.658 ± 0.06 by 114 standard deviations. These indicators show that our photon source has the characteristics of high brightness with high entanglement visibility, which meets well our goals.

Keywords

Quantum physics, Quantum information, Quantum communication, Quantum optics, Spontaneous Parametric Down-Conversion, Entangled photonic source

Abstract

Kvantoptik är ett snabbt växande område som involverar många delfält, till exempel kvantinformation, kvantnyckelfördelning, kvantteleportation och kvantberäkning. I denna bakgrund är en intrasslad fotonkälla med hög ljusstyrka nyckeln till framgången för kvantexperiment. Dessutom är telekombandet mycket vänligt för omkonfigurering och sammanlänkning mellan olika fotoniska plattformar.

I detta projekt studerar vi teorin om spontan parametrisk nedkonvertering (SPDC) och egenskapen hos periodiskt polad kaliumtitanylfosfat (PPKTP). Vi bygger en intrasslad källa med hög ljusstyrka med Sagnac-interferometern och testar beteendet.

Vi använder den högeffektiva supraledande nanotråds-singelfotondetektorn (SNSPD) för att detektera fotonerna, och vi använder quTAG-tidstaggaren för att samla sammanfallsfrekvensen. Ljusstyrkan är en halv miljon per sekund för enkel väg och koincidensfrekvensen är 60k per sekund. Synligheten i $|H\rangle$ och $|+\rangle$ basis är 97.7% och 87.2%, vilket bryter mot CHSH med erhållet S värde 2.658 ± 0.06 med 114 standardavvikelser. Dessa indikatorer visar att vår fotonkälla har egenskaperna hög ljusstyrka och hög intrassling, vilket väl uppfyller våra mål.

Nyckelord

Quantum physics, Quantum information, Quantum communication, Quantum optics, Spontaneous Parametric Down-Conversion, Entangled photonic source

Acknowledgements

First I would like to thank my senior fellow apprentice and supervisor Dr. Jun Gao for his guidance in experimental skills patiently, especially the fine adjustment of the light path like magic. What's more, is his profound knowledge on the usages of different components and the deep understanding of projective measurement in quantum optics also helps me a lot.

Then, I would like to thank my supervisor Associate Professor Dr. Ali Elshaari for kind arrangement of the experiment project. He is always open for discussing the most advanced technology and carrying out the state of art research. This project would not have been started without his inputs and enthusiasm.

Furthermore I want to thank the group leader Professor Dr. Val Zwiller. He arranged the lab with a great environment. Prof. Zwiller always lead the frontier of quantum photonics, and he is very generous of purchasing the top equipment.

I would like to thank Dr.Samuel Gyger for his advice on the operation of superconducting nanowire single-photon detector (SNSPD). I would like to thank Ph.D student Theodor Staffas for his advice on the laser and the cooling system. I also want to thank all other members in QNP group for their help and a very pleasant atmosphere we contribute together.

Finally I want to thank my parents for their financial and emotional Support. Their generosity enables me to focus on this research project.

Contents

Chapter 1

Introduction

Quantum information is a rapidly developing subject based on the theory of quantum physics, where information is physically encoded in the state of a quantum system. In 1935, Schrödinger showed the quantum entanglement is a natural state for a quantum system [1], which means that by manipulating the quantum entanglement, we can manipulate the information to be processed or transported.

Compared with other platforms such as superconducting quantum circuits, quantum optics using photons meets the requirement for long distance communication and perseverance of quantum coherence, thanks to the weak interaction of photons with environment, with first experimental demonstration in 1997 [2]. Another important property is that we can manipulate the states of photons easily. For example, only with several polarization beam splitters and waveplates we can engineer the quantum states we desire [3].

With the advantages we listed, it is worth noting that our task can be divided into two parts: High brightness and telecom band quauntum source. The information per second the source can send depends on the photon counts per second the source can generate. We can understand this better by thinking of how our life changed with the internet speeds increasing from 1KB/s decades ago to 100 MB/s currently . Similarly, high brightness is a vital feature for an advanced entangled source. On the other side, 1550 nm telecom band light is widely used in modern fiber communication with high compatibility and low propagation loss of optical fibers[4], and these are the reasons of why we prefer this wavelength range.

In this project we focus on build a high brightness telecom band entangled photon

source based on the Sagnac interferometer and Periodically poled potassium titanyl phosphate (PPKTP) crystal. We use a 780 nm pulsed laser to pump the nonlinear crystal and get 1550 nm spontaneous parametric down-conversion (SPDC) photon pairs.

This report is divided to the following main parts, with brief summary presented below for each chapter:

Chapter 2, *Background*, introduces the basics concepts and relevant formulas of entangled source.

Chapter 3, *Experiment*, introduces the build of the optical path and the coincidence measurement.

Chapter 4, *Data analysing*, analyse the measured data and the quality of this source.

Chapter 5, *Conclusion and Future outlook*, sums up the results we obtained, and explores the next step we can do with this source.

Chapter 2

Background

2.1 Quantum superposition and entanglement

2.1.1 Quantum superposition

As a fundamental principle of quantum mechanics, quantum superposition [5] illustrates that a quantum state can be represented as a sum of basis states due to the linear property of Schrödinger equation. A quantum system can be described by:

$$|\psi\rangle = \sum_x C(x)|x\rangle \tag{2.1}$$

where $|x\rangle$ refers to the different basis quantum states and the $C(x)$ refers to the corresponding probability amplitude. The square of this amplitude indicates the probability of finding the state in the quantum system, with the relationship:

$$\sum_x |C(x)|^2 = 1 \tag{2.2}$$

A good example of quantum superposition in real experiment is the superposition of the polarization of a photon [6]. We define the horizontal polarization as $|H\rangle$ and the vertical polarization as $|V\rangle$, then a photon polarized along $+45^\circ$ reads as:

$$|+\rangle = \frac{1}{\sqrt{2}}(|H\rangle + |V\rangle) \tag{2.3}$$

Quantum non-cloning theorem guarantees the security of quantum communication

[7]. Imagine we have the initial system:

$$|\psi\rangle = \frac{1}{\sqrt{2}}(|0\rangle + |1\rangle) \tag{2.4}$$

A cloning operator U which is unitary must have the following functions:

$$\begin{aligned} U|0\rangle|0\rangle &= |0\rangle|0\rangle \\ U|1\rangle|0\rangle &= |1\rangle|1\rangle \end{aligned} \tag{2.5}$$

If we apply U to the initial system it should be:

$$|\psi'\rangle = \mathbf{U}|\psi\rangle = \mathbf{U}\left[\frac{1}{\sqrt{2}}(|0\rangle + |1\rangle)\right]|0\rangle = \frac{1}{2}(|0\rangle + |1\rangle)(|0\rangle + |1\rangle) \tag{2.6}$$

However, according to the quantum superposition we have:

$$|\psi'\rangle = \mathbf{U}\left[\frac{1}{\sqrt{2}}(|0\rangle + |1\rangle)\right]|0\rangle = \frac{1}{\sqrt{2}}(U|0\rangle|0\rangle + |1\rangle|0\rangle) = \frac{1}{\sqrt{2}}(|0\rangle|0\rangle + |1\rangle|1\rangle) \tag{2.7}$$

They are paradoxical, and point out that it is impossible to create an independent and identical copy of an arbitrary quantum state without disturbing it. This property is the origin of the advantage of quantum information.

2.1.2 Quantum entanglement

Quantum entanglement is a physical phenomenon that the particles in a system are highly correlated such that the quantum state of each particle cannot be described independently from the state of the others, even if they are separated by a large distance. This property is considered as Non-local correlation which had been tested in 2015 [8]. Position, momentum, spin, and polarization are some typical physical quantities, which had been founded to be entangled in real systems.

From theoretical viewpoint, consider a system consisting of two subsystems. The Hilbert space of the composite system is then the tensor product of these two subsystems:

$$H = H_A \otimes H_B \tag{2.8}$$

And any vectors in the Hilbert space H can be written as the tensor product of vectors $|\psi\rangle_A$ and $|\psi\rangle_B$ in the Hilbert spaces H_A and H_B:

$$|\psi\rangle = |\psi\rangle_A \otimes |\psi\rangle_B \tag{2.9}$$

The systems can be represented in this formalism are called separable system. However, sometimes the system can not be separated as the tensor products of several subsystems, for example, the Bell states [9]:

$$\begin{aligned}
\left|\Phi^+\right\rangle &= \frac{1}{\sqrt{2}}\left(|0\rangle_A \otimes |0\rangle_B + |1\rangle_A \otimes |1\rangle_B\right) \\
\left|\Phi^-\right\rangle &= \frac{1}{\sqrt{2}}\left(|0\rangle_A \otimes |0\rangle_B - |1\rangle_A \otimes |1\rangle_B\right) \\
\left|\Psi^+\right\rangle &= \frac{1}{\sqrt{2}}\left(|0\rangle_A \otimes |1\rangle_B + |1\rangle_A \otimes |0\rangle_B\right) \\
\left|\Psi^-\right\rangle &= \frac{1}{\sqrt{2}}\left(|0\rangle_A \otimes |1\rangle_B - |1\rangle_A \otimes |0\rangle_B\right)
\end{aligned} \tag{2.10}$$

If we measure the two qubits in this system, they would be completely correlated for $|\Phi\rangle$ and anti-correlated for $|\Psi\rangle$.

2.2 Projective measurement

We introduce a Herimitian operator (observable) on the state space of the system being observed M to describe the projective measurement, and the observable can be written in a spectral decomposition [10]:

$$M = \sum_m m P_m \tag{2.11}$$

P_m is the projector, m is the corresponding eigenvalue. Now the probability of getting result m when we measure quantum state $|\psi\rangle$ is:

$$p(m) = \langle\psi| P_m |\psi\rangle \tag{2.12}$$

After the measurement, the quantum state itself immediately collapses to:

$$\frac{P_m|\psi\rangle}{\sqrt{p(m)}} \tag{2.13}$$

The average values for this projective measurement is:

$$\begin{aligned}\mathbf{E}(M) &= \sum_m mp(m) \\ &= \sum_m m \langle\psi| P_m |\psi\rangle \\ &= \left\langle \psi \middle| \left(\sum mP_m\right) \middle| \psi \right\rangle \\ &= \langle\psi|M|\psi\rangle.\end{aligned} \tag{2.14}$$

For our entangled photon pairs , we can write the Herimitian operator as a 4×4 matrix.

2.3 Spontaneous parametric down-conversion

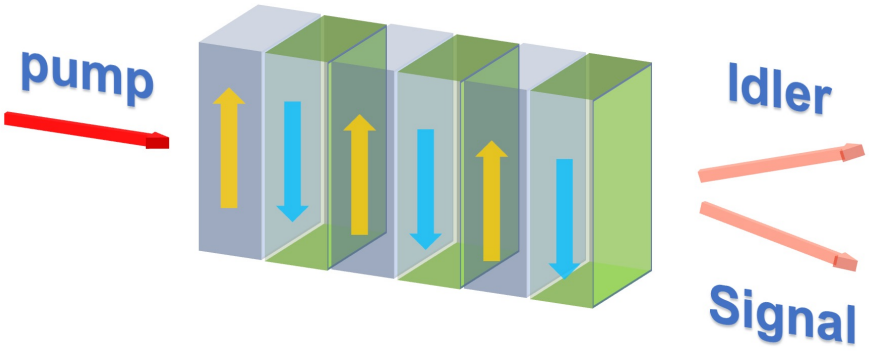

Figure 2.3.1: **SPDC process based on ppktp crystal:** The ppktp crystal interacts with one pump photon, and generates idler photon together with signal photon, which obeys the law of conservation of energy and law of conservation of momentum.

Spontaneous parametric down-conversion (SPDC) is a nonlinear optical process which was realized in 1967 [11], it produces a pair of photons from one pump photon. it is a three-wave mixing process with second-order nonlinear effect. From an engineering point of view, SPDC is a mature technique to generate high quality entangled source.

According to the law of conservation of energy and the law of conservation of momentum , the total energy and total momentum of the photon pair are equal to the energy and momentum of the pump photon. From the law of conservation of energy, we can get,

$$\omega_p = \omega_s + \omega_i \tag{2.15}$$

where ω_p, ω_s, ω_i are the angular frequencies of pump photons, signal photons, and idle photons. From the law of conservation of momentum, we can get,

$$\mathbf{k}_p = \mathbf{k}_s + \mathbf{k}_i \tag{2.16}$$

where $\mathbf{k}_p$, $\mathbf{k}_s$, $\mathbf{k}_i$ are the wavenumber vectors of pump photons, signal photons, and idle photons, respectively.

It is important to notice that the refractive index changes with frequency, and only certain triplets of frequencies could be phase-matched. Birefringent nonlinear materials, whose refractive index varies with polarization, are most frequently used to accomplish phase-matching. We can categorize different types of SPDC processes by the polarizations of the input photon (pump) and the two output photons (signal and idler)[12]:

1.Type-0 SPDC: the pump photon has the same polarization as the signal and idler photons.

2.Type-I SPDC: the signal and idler photons share the same polarization to each other and orthogonal to the pump polarization.

3.Type-II SPDC: the signal and idler photons have orthogonal polarization.

In this project we use Type-II SPDC to produce photons. The linear orbits describing the emission of the photon pairs are contained in two conical surfaces, as shown in the 2.3.2, one conical surface contains the horizontally polarization polarized signal, the other conical surface contains the vertically polarized idler orbit. At the intersection of the two conical surfaces are two straight lines. Two photons whose orbits are on these two lines can have horizontal polarization or vertical polarization. If one photon has horizontal polarization, the other has vertical polarization; and vice versa. It is impossible to identify which photon has horizontal polarization and which photon

has vertical polarization without measurement. Therefore, these two photons with perpendicular polarizations are entangled with each other, and the entangled state is:

$$\left(|H\rangle_1|V\rangle_2 + |V\rangle_1|H\rangle_2\right)/\sqrt{2} \tag{2.17}$$

where $|H\rangle$ is the horizontal polarization, $|V\rangle$ is the vertical polarization. In real experiment, the path difference would result in a phase shift and contribute a phase factor ϕ, so the entangled state reads:

$$\left(|H\rangle_1|V\rangle_2 + e^{i\phi}|V\rangle_1|H\rangle_2\right)/\sqrt{2} \tag{2.18}$$

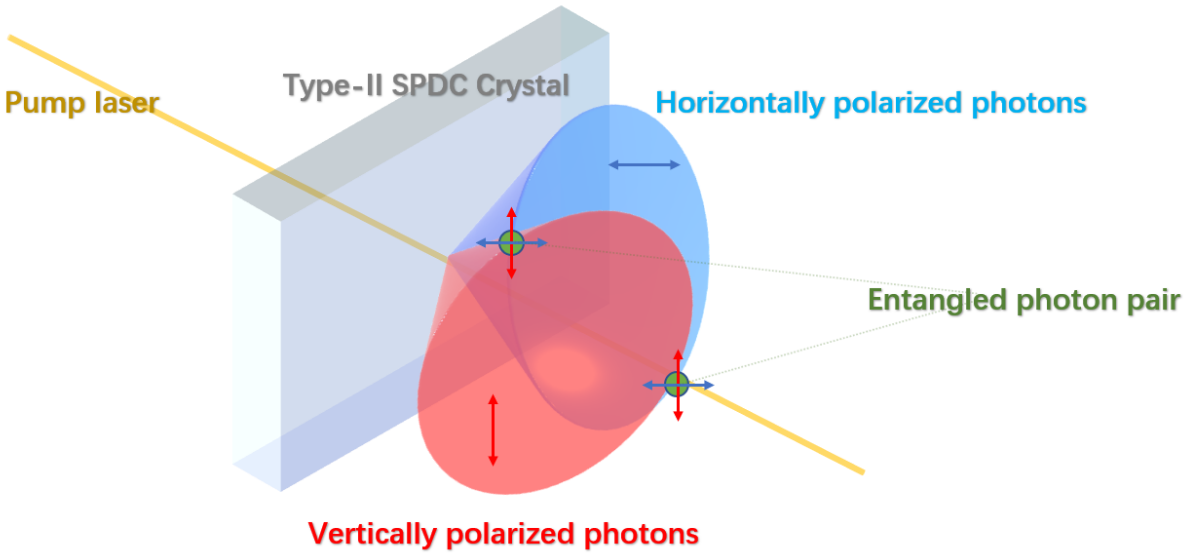

Figure 2.3.2: **A type-II SPDC process:** The crystal interacts with one pump photons, generates entangled photon pairs with orthogonal polarizations.

2.4 Quasi-phase-matching and PPKTP crystal

Quasi -phase-matching is an important technique which was introduced in 1962 [13] for nonlinear optical frequency conversion, it allows a positive net flow of energy from the pump to the signal and idler by producing a a periodic structure in the nonlinear crystal.

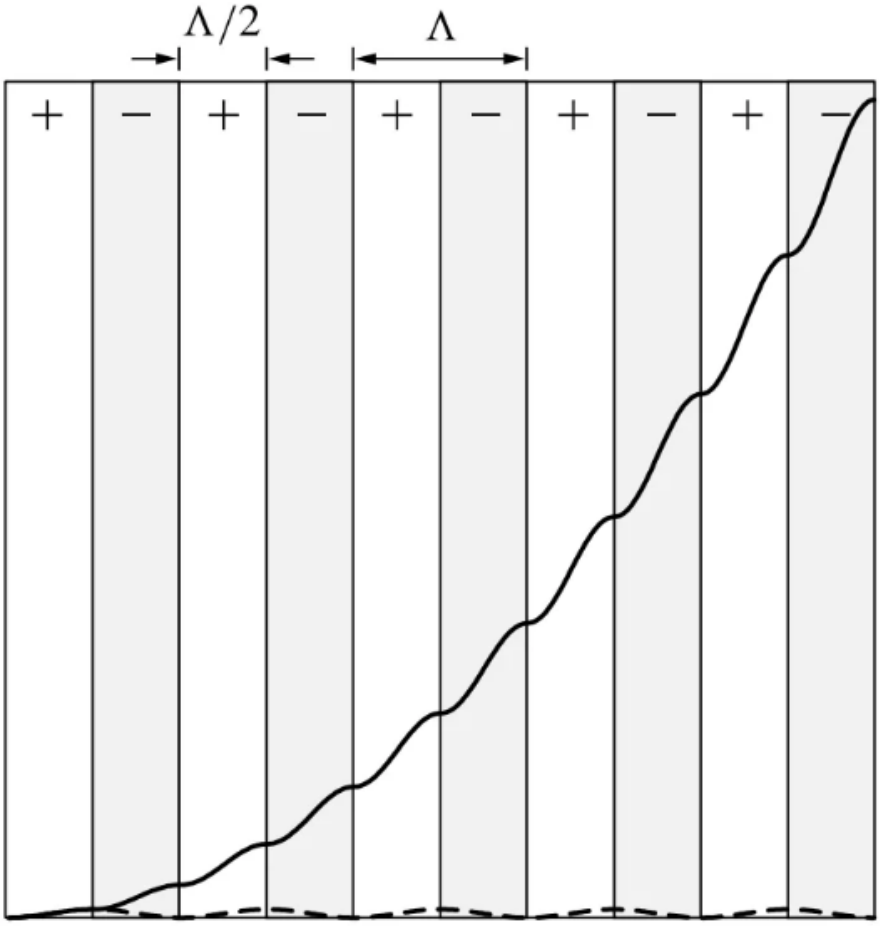

Figure 2.4.1: **A schematic of quasi-phase-matching:** The dashed line shows the intensity evolution along the interaction distance of no phase matching condition, the solid line shows the intensity evolution along the interaction distance of quasi-phase-matching condition.

The phase mismatch in a nonlinear crystal can be described as:

$$\Delta\mathbf{k} = \mathbf{k}_1 + \mathbf{k}_2 - \mathbf{k}_3 \tag{2.19}$$

And the existence of this phase mismatch result in a change of the phase φ by an amount of π over a coherence length as the 2.4.1 shows, resulting in a change of sign in and a reversal of the direction of energy flow in this whole process. However, if we periodically modulate the susceptibility such that a phase $\varphi_\chi = \pi$ is introduced over each coherence length, the total phase φ can be reset to its initial value so that the positive net flow of energy is achieved, as the solid line indicates. Λ is the modulation period, and

$$\Lambda = 2\frac{\pi}{|\Delta k|} \tag{2.20}$$

The intensity of generated photons have the following form [14]:

$$I \propto e^{-\Delta kL} L^2 \operatorname{sinc}^2\left(\frac{\Delta kL}{2}\right) \tag{2.21}$$

where L is the crystal length along the interaction direction.

PPKTP is periodically poled potassium titanyl phosphate, which was studied and shown to have optical properties for quasi-phase-matching in 1976 [15]. Compared with BBO crystal, PPKTP has higher second-order nonlinear effect. The PPKTP crystal belongs to the orthogonal crystal system, since the direction of the pump light is consistent with the optical axis (or orthogonal), there is no walk-off effect of the down-conversion photons even if the crystal length is long, and the phase factor ϕ can be minimized. We can also tune the SPDC frequencies for the crystal by using thermal control to reach a selected certain telecom band.

2.5 Sagnac interferometer

The previous setup for entangled source based on PPKTP is Mach-Zehnder interferometer as the figure 2.5.1 shows which was proposed by Marco Fiorentino in 2004 [16].

However, this setup is limited by the phase stability. To overcome this challenge, a new setup as shown in figure 2.5.2 was proposed by Franco N. C. Wong in 2006 [17] to pump the PPKTP crystal in two opposite directions. This setup has been able to produce high entanglement quality while also permitting a high source brightness since this method uses collinear down-conversion and does not require phase stabilization.

The core part is a Isosceles right triangle in this Sagnac interferometer, and the PPKTP crystal is placed in the middle of the base of the triangle. A pump photon propagates along the blue path, as it is reflected by a Dichroic mirror (this DM will transmit the idler and signal photons) as the figure 2.5.2 shows:

(a) For H-polarized pump $|H\rangle$, the photon is transmitted in the PBS and go in the anti-clock path, the photon interact with the PPKTP crystal and generates H-polarized

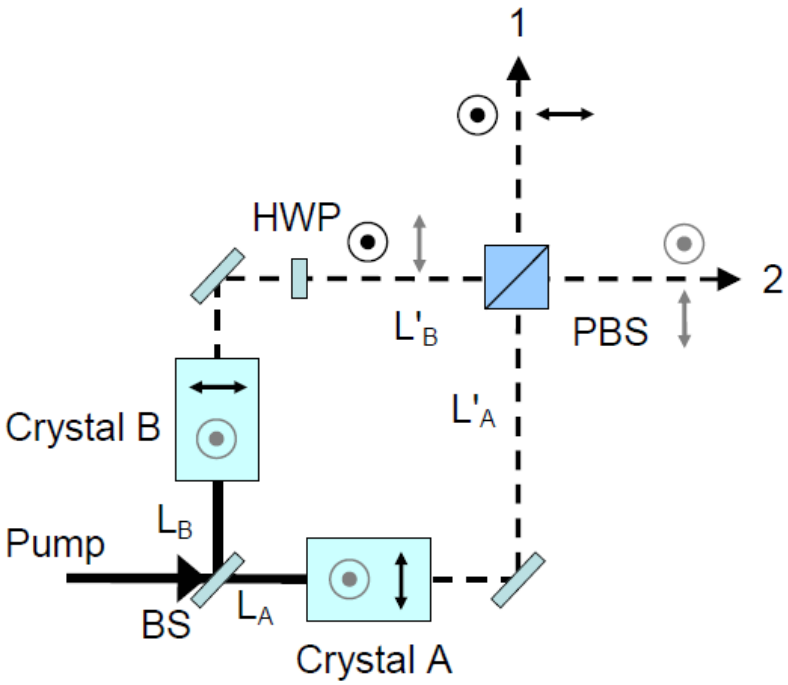

Figure 2.5.1: **A schematic of Mach-Zehnder interferometer (from [16]):**

signal photon and V-polarized idler photon, the state can be written as $|H_s\rangle|V_i\rangle$ in the red path. After the mirror and the HWP, the state becomes $|V_s\rangle|H_i\rangle$. The H-polarized idler photon transmitted by the PBS and reaches path 2, while the V-polarized photon reflected by the PBS and reaches path 1, the final state is $|V_s\rangle_1|H_i\rangle_2$.

(b) For V-polarized pump $|V\rangle$, the photon is reflected in the PBS and go in the clock-wise path, the photon interact with the PPKTP crystal and generates H-polarized signal photon and V-polarized idler photon, the state can be written as $|H_s\rangle|V_i\rangle$ in the red path. After the mirror, the state becomes $|H_s\rangle|V_i\rangle$. The H-polarized idler photon transmitted by the PBS and reaches path 1, while the V-polarized photon reflected by the PBS and reaches path 2, the final state is $|H_s\rangle_1|V_i\rangle_2$.

The final output state is the superposition of (a) and (b), by controlling the ratio of Horizontal and Vertical polarized pump photons, and rotating the HWP, we can produce the entangled superposition state that we want:

$$\sin\alpha\,|H_s\rangle_1\,|V_i\rangle_2 + e^{i\varphi}\cos\alpha\,|V_s\rangle_1\,|H_i\rangle_2 \tag{2.22}$$

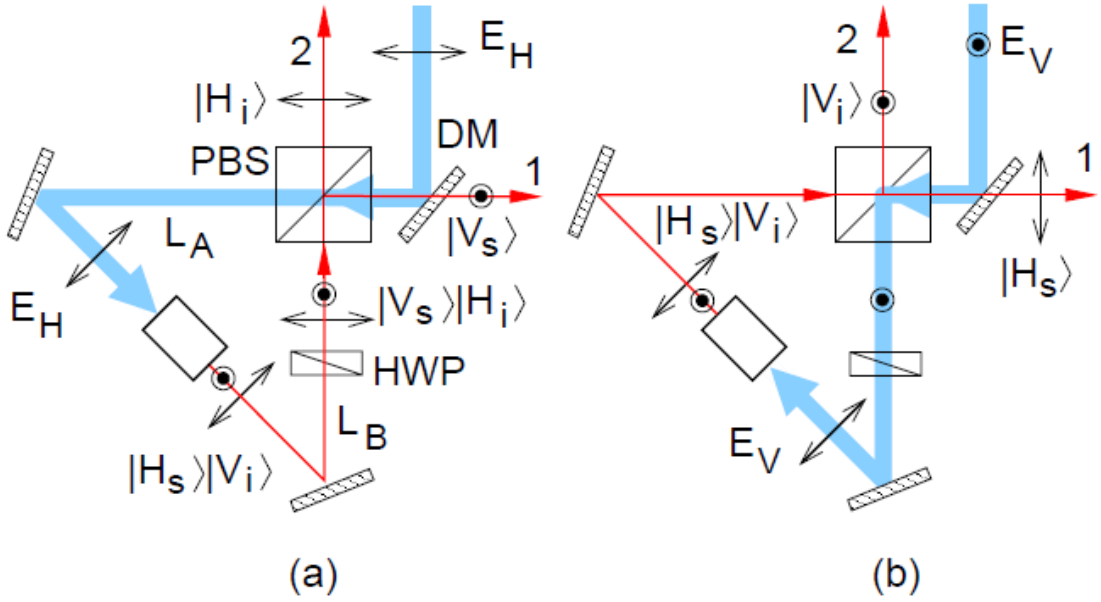

Figure 2.5.2: **A schematic of Sagnac interferometer (from [17]):** (a) H-polarized input (b) V-polarized input

Chapter 3

Experiment

3.1 Setup

The experimental setup is shown in figure 3.1.1. We employ a 780 nm pulsed laser to pump the PPKTP crystal. The part A in the blue dotted box is made of a quarter-wave plate, a half-wave plate and a polarized beam splitter which transmits horizontally polarized photons and reflects the vertically polarized ones. The quarter-wave plate and the half-wave plate in part A are working for maximizing the transmittance of the PBS by adjusting them.

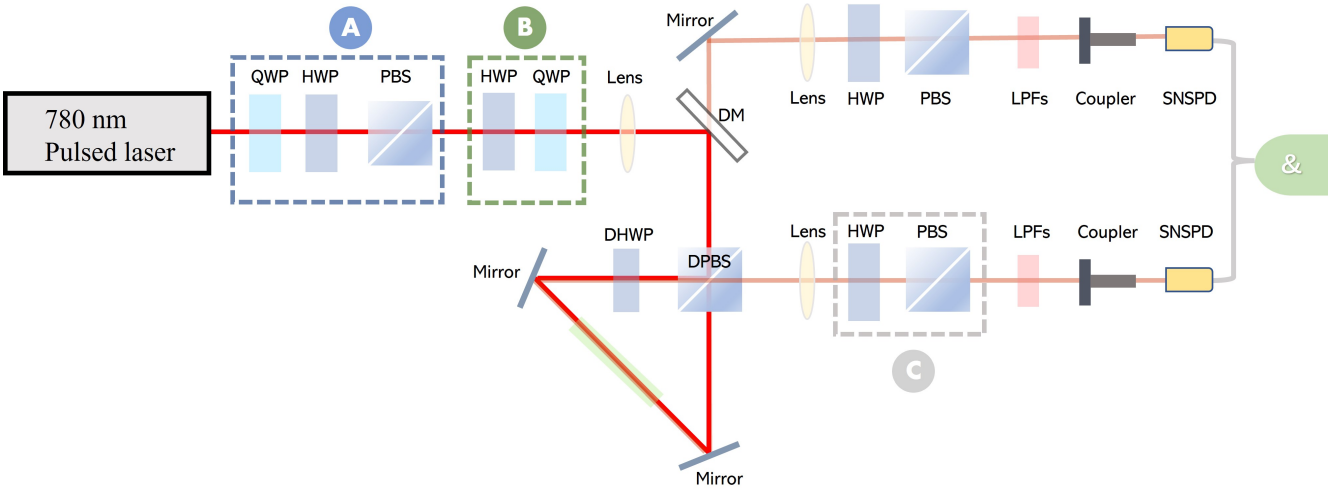

Figure 3.1.1: **A schematic of the setup of the entangled source**

After part A, we have fully H-polarized pump light. The part B in the green dotted box is made of a half-wave plate and a quarter-wave plate. The H-polarized light is incident on the half-wave plate, the polarization direction is changed, and the light

transmitted from the half-wave plate is then incident on the quarter-wave plate. When the polarization direction of the linearly polarized light is consistent with the fast axis or slow axis of the quarter-wave plate, the outgoing light is linearly polarized. In this condition the half-wave plate can be used to adjust the linear polarization direction. When the polarization direction is inconsistent with both the fast and slow axis, the outgoing light is elliptically polarized or circularly polarized. At this time, the quarter-wave plate can be used to adjust the ellipticity and handedness. In conclusion, we can generate any polarized states based on the combination of a half-wave plate and a quarter-wave plate in part B.

The light after part B is collimated by a $f = 200$ mm lens and reflected by a dichroic mirror (transmits the 780 nm light and reflects the 1560 nm light), and guided into the sagnac-loop. The sagnac-loop consists of a dual-wavelength polarized beam splitter (DPBS), a dual-wavelength half-wave plate (DHWP), two mirrors and a PPKTP crystal. The PPKTP crystal is installed in a thermal control stage which shown in figure 3.1.2. The temperature is maintained to achieve a degenerate wavelength at 1560 nm.

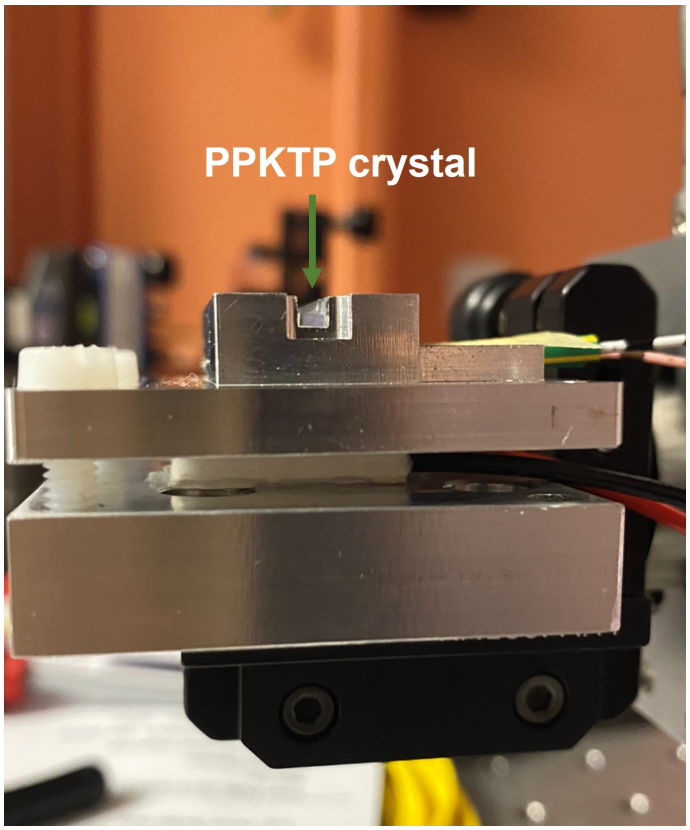

Figure 3.1.2: **The picture of PPKTP crystal installed in a thermal control stage**

The PPKTP crystal was pumped simultaneously by clockwise

(CW) and counterclockwise (CCW) laser pulses. The DHWP is set at 45 degrees to transform the V-polarized light into H-polarized in the CCW path. As a result, both the CW and CCW pulses are H-polarized as well as focused in the middle of the PPKTP crystal, and the down-converted photons are collimated by two $f = 300$ mm lenses to fiber couplers through a long pass filter.

To test the polarization correlation, we add the combination of a HWP and a PBS in the gray dotted box as part C. This part works as a polarizer. By setting the angles θ_1 and θ_2 in path 1 and path 2, we can perform a series of polarization correlation measurements. The picture of the complete setup is shown in figure 3.1.3.

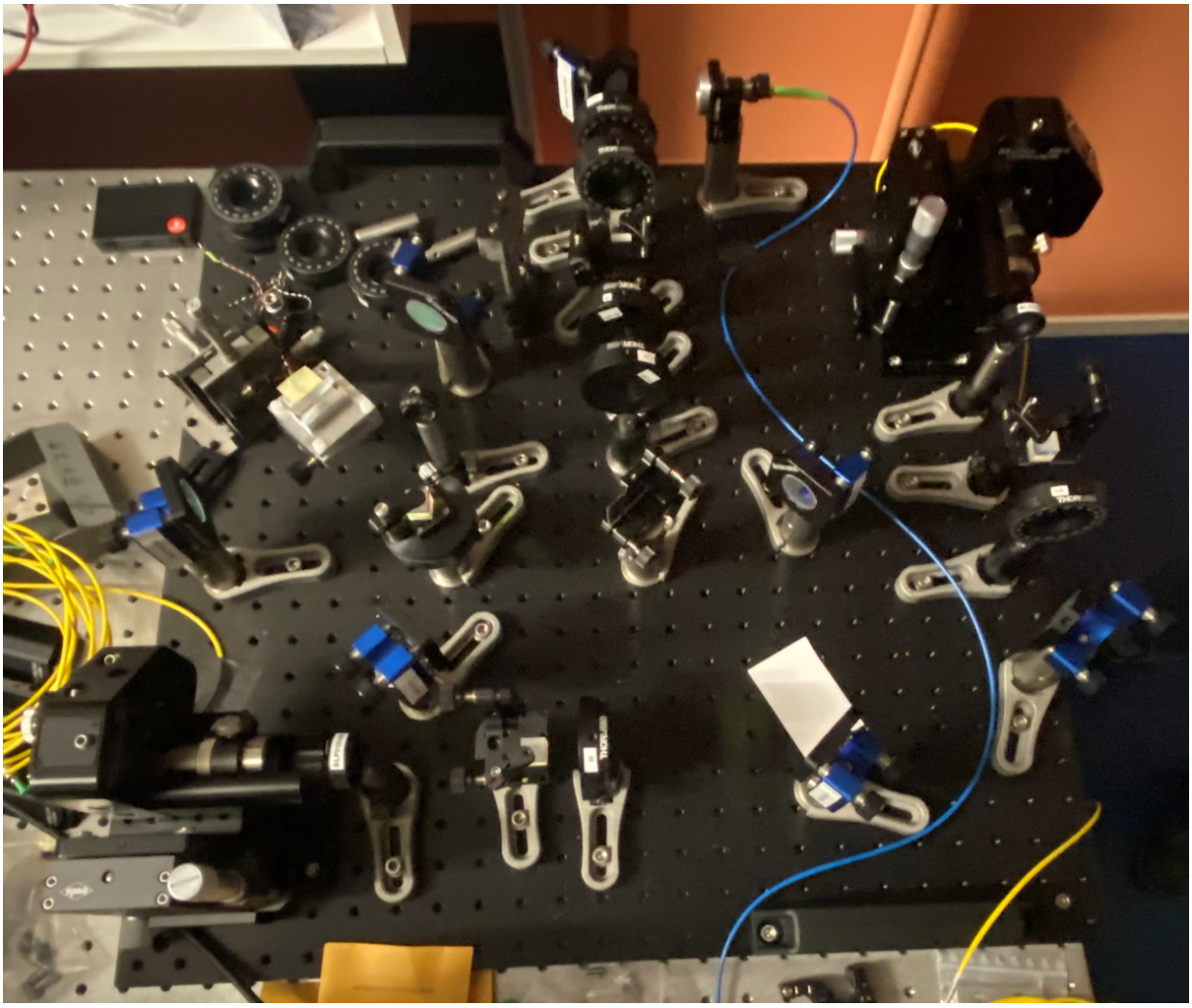

Figure 3.1.3: **The picture of optical path setup**

3.2 Measurement

We employ the Single Quantum SNSPD as shown in figure 3.2.1b) with high detection efficiency of 76% and high timing resolution 30 picoseconds [18, 19] to measure the single photon counts in path 1 and path 2. With a 120 mW pump power for the PPKTP crystal, the single photon counts for each path is 500 kcps, the background counts have been subtracted.

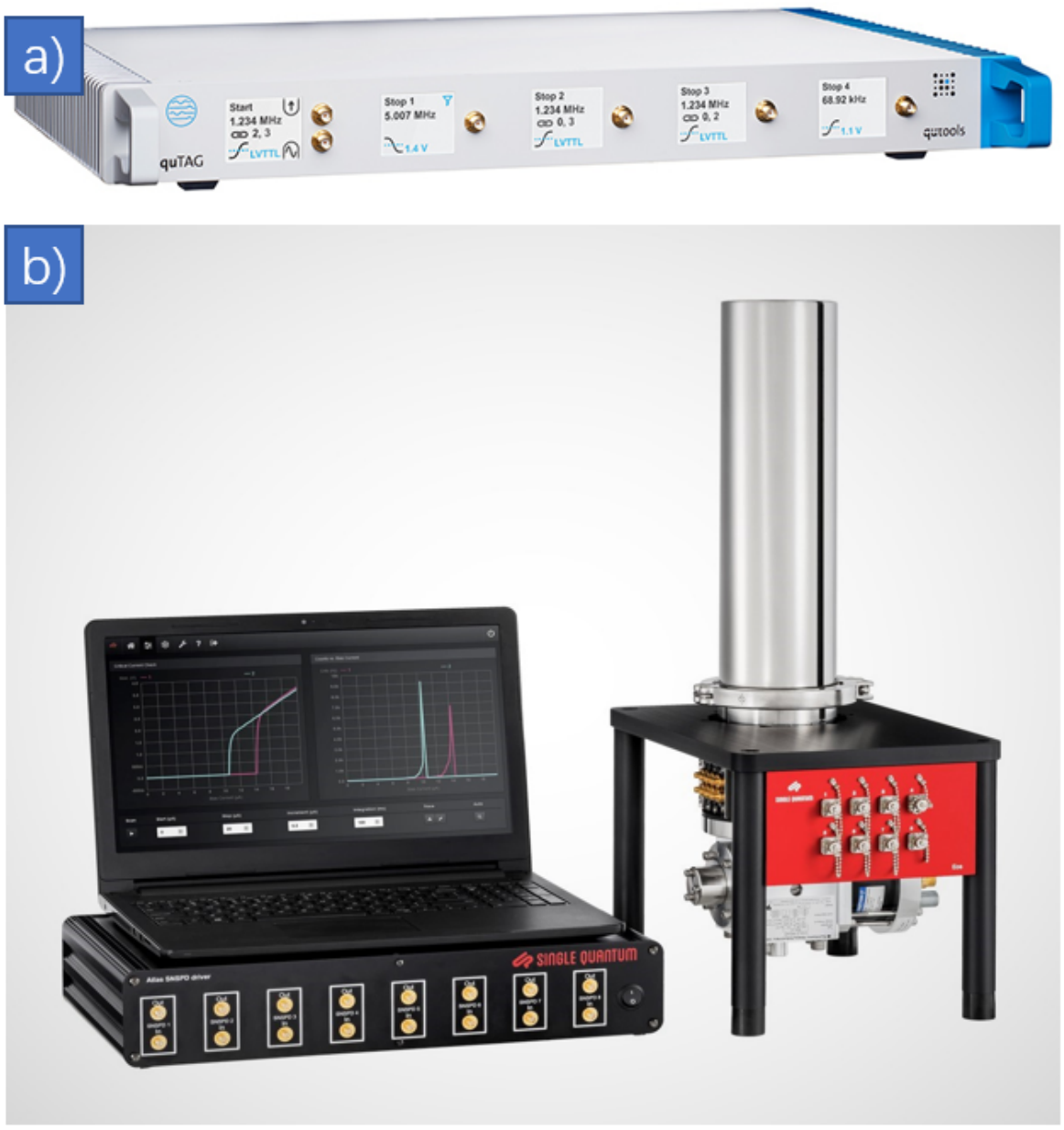

Figure 3.2.1: **a) The picture of quTAG time tagger. b) The picture of Single Quantum SNSPD**

We fix the pump power and carry out a polarization correlation measurement by

quTAG time tagger as shown in figure 3.2.1a) with $|H\rangle$ basis and $|+\rangle = \frac{1}{\sqrt{2}}(|H\rangle + |V\rangle)$ basis respectively. The result is recorded in table 3.2.1.

Degree	$\|H\rangle$ basis	$\|+\rangle$ basis
0	1028	35k
10	948	25k
20	4673	16k
30	11k	9236
40	20k	5089
50	30k	3703
60	40k	5788
70	49k	11k
80	56k	18k
90	59k	27k
100	59k	35k
110	55k	44k
120	49k	50k
130	39k	53k
140	29k	54k
150	19k	51k
160	9891	47k
170	3650	40k
180	688	31k

Table 3.2.1: Coincidence counts in one second with degrees from 0 to 180 under $|H\rangle$ basis and $|+\rangle$ basis.

Chapter 4

Data Analysis

4.1 Correlation measurement

We plot the data in table 3.2.1 as shown in figure 3.2.1. The blue curve is the coincidence counts in the $|H\rangle$ basis, the grey curve is the coincidence counts in the $|+\rangle$ basis.

Recalling the equation 2.22, we set $\alpha = 0$ and $\varphi = \pi$, the entangled photon pair in this Sagnac interferometer can be expressed as $|\Psi\rangle = \frac{1}{\sqrt{2}}(|V\rangle_1|H\rangle_2 - |H\rangle_1|V\rangle_2)$

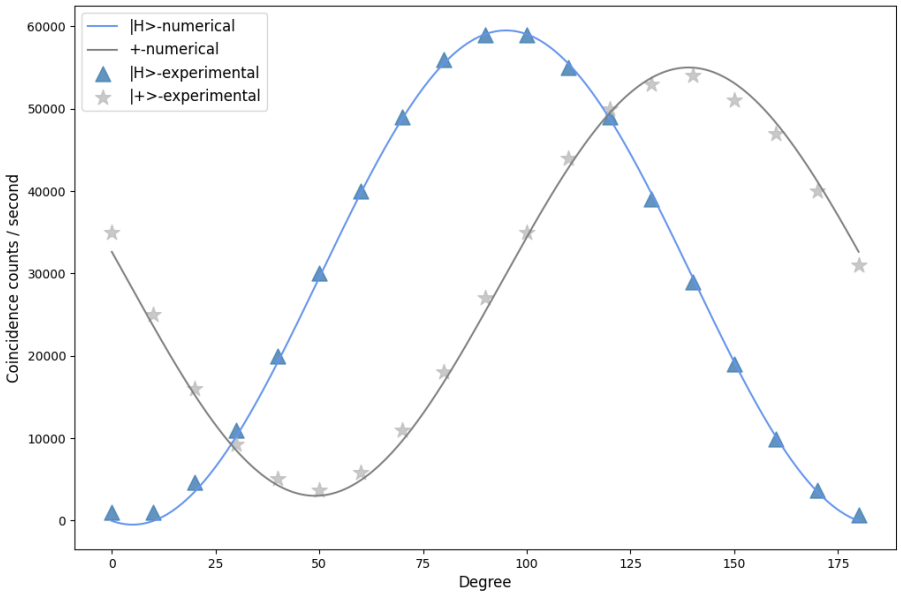

Figure 4.1.1: **Coincidence counts in one second as a function of the two polarizers**

The polarizers settings at polarization angles a and b have the bases:

$$\begin{aligned} |V\rangle_1 &= \cos(a)|V\rangle - \sin(a)|H\rangle \\ |H\rangle_1 &= \sin(a)|V\rangle + \cos(a)|H\rangle \\ |V\rangle_2 &= \cos(b)|V\rangle - \sin(b)|H\rangle \\ |H\rangle_2 &= \sin(b)|V\rangle + \cos(b)|H\rangle \end{aligned} \tag{4.1}$$

The probability of coincidence detection for one pair of photons is:

$$P = |\left\langle H|_1 \langle H|_2 \mid \Psi\right\rangle|^2 \tag{4.2}$$

When we measure the coincidence counts under $|H\rangle$ and set the polarization angle for path 1 to a=$0°$, $|H\rangle_1 = |H\rangle$, $|H\rangle_2 = \sin(b)|V\rangle + \cos(b)|H\rangle$, P can be calculated as following:

$$P_H = |\left\langle H|_1 \langle H|_2 \mid \Psi\right\rangle|^2 = |\langle H|\frac{1}{\sqrt{2}}(\sin(b)|H\rangle - \cos(b)|V\rangle)|^2 = \frac{\sin(b)^2}{2} = \frac{1-\cos(2b)}{4} \tag{4.3}$$

When we measure the coincidence counts under $|+\rangle$ and set the polarization angle for path 1 to a=$45°$, $|+\rangle_1 = \frac{1}{\sqrt{2}}|H\rangle + \frac{1}{\sqrt{2}}|V\rangle$, $|+\rangle_2 = \sin(b)|V\rangle + \cos(b)|H\rangle$, P can be calculated similarly:

$$P_+ = |\left\langle +|_1 \langle +|_2 \mid \Psi\right\rangle|^2 = |\frac{1}{\sqrt{2}}(\langle H| + \langle V|)\frac{1}{\sqrt{2}}(\sin(b)|H\rangle - \cos(b)|V\rangle)|^2 = \frac{1-\sin(2b)}{4} \tag{4.4}$$

In figure 4.1.1 we can identify that the maximum and the minimum of the grey curve has a $\frac{\pi}{4}$ phase shift compared with the blue curve, in agreement with the theory.

The visibilities under $|H\rangle$ basis and $|+\rangle$ basis are defined as:

$$\begin{aligned} \text{Visibility}_H &= \frac{N_{HV} - N_{HH}}{N_{HV} + N_{HH}} \\ \text{Visibility}_+ &= \frac{N_{+-} - N_{++}}{N_{+-} + N_{++}} \end{aligned} \tag{4.5}$$

From equation 4.5 we can calculate that $\text{Visibility}_H = 97.7\%$, $\text{Visibility}_+ =$

87.2%.

4.2 CHSH inequality

The CHSH inequality, developed by Clauser, Horne, Shimony and Holt [20], is most used in experiments to test the hidden variable theory for quantum mechanism.

We assume the existence of a hidden variable λ which includes the complete information for each photon [21]. It has a distribution $\rho(\lambda)$ with properties $\rho(\lambda) \geq 0$ and $\int \rho(\lambda)d\lambda = 1$ to describe the measurement resultsn :

$$< O >= \int O(\lambda)\rho(\lambda)d\lambda \tag{4.6}$$

According to the locality assumption, if we measure the polarization of photon A along direction $\vec{a}$, and measure the polarization of photon B along direction $\vec{b}$, the measurement results are independent of each other, and the expectation of the correlation function reads:

$$E(\vec{a}, \vec{b}) = \int A(\vec{a}, \lambda)B(\vec{b}, \lambda)\rho(\lambda)d\lambda \tag{4.7}$$

The difference between expectations of the correlation at different polarization bases can be scaled with:

$$\begin{aligned} &|E(a,b) - E\,(a,b')| \\ &\leq \int |A(a,\lambda)B(b,\lambda) - A(a,\lambda)B\,(b',\lambda)|\,\rho(\lambda)d\lambda \\ &\leq \int |A(a,\lambda)\,[B(b,\lambda) - B\,(b',\lambda)]|\,\rho(\lambda)d\lambda \\ &\leq \int |B(b,\lambda) - B\,(b',\lambda)|\,\rho(\lambda)d\lambda \end{aligned} \tag{4.8}$$

and similarly:

$$\begin{aligned} &|E\,(a',b) + E\,(a',b')| \\ &\leq \int |B(b,\lambda) + B\,(b',\lambda)|\,\rho(\lambda)d\lambda \end{aligned} \tag{4.9}$$

The definition of S is $S \equiv |E(a,b) - E(a,b')| + |E(a',b) + E(a',b')|$, clearly we have:

$$\begin{aligned} S \leq \int & (|B(b,\lambda) - B(b',\lambda)| \\ & + |B(b,\lambda) + B(b',\lambda)|)\, \rho(\lambda) d\lambda \end{aligned} \tag{4.10}$$

Since $|B(b,\lambda)| \leq 1$ and $|B(b',\lambda)| \leq 1$,

$$S \leq \int 2\rho(\lambda) d\lambda = 2 \tag{4.11}$$

However, if the entanglement interpretation is right, the CHSH inequality would be violated and the value S obeys:

$$2 \leq S \leq 2\sqrt{2} \tag{4.12}$$

Experimentally, the correlation function reads:

$$E(a,b) = \frac{N(a,b) + N\left(a+\frac{\pi}{2}, b+\frac{\pi}{2}\right) - N\left(a+\frac{\pi}{2}, b\right) - N\left(a, b+\frac{\pi}{2}\right)}{N(a,b) + N\left(a+\frac{\pi}{2}, b+\frac{\pi}{2}\right) + N\left(a+\frac{\pi}{2}, b\right) + N\left(a, b+\frac{\pi}{2}\right)} \tag{4.13}$$

In this experiment we choose:

$$a = -22.5^\circ, a' = 22.5^\circ, b = -45^\circ, b' = 0^\circ \tag{4.14}$$

The coincidence counts per second we collected are shown in the following table:

Bob / Alice	22.5°	112.5°	67.5°	-22.5°
0°	3131	31000	27000	7678
90°	30000	3759	6241	29000
45°	6898	25000	4853	30000
-45°	22000	8405	26000	3150

(4.15)

Then we can calculate the correlation functions using the coincidence counts we directly measured:

$$
\begin{aligned}
E(a,b) &= E(-22.5^\circ, -45^\circ) = -0.749917973 \\
E(a,b') &= E(-22.5^\circ, 0^\circ) = 0.601853573 \\
E(a',b) &= E(22.5^\circ, -45^\circ) = -0.508755598 \\
E(a',b') &= E(22.5^\circ, 0^\circ) = -0.797024599
\end{aligned}
\tag{4.16}
$$

The obtained S value is 2.658 ± 0.006 (114 σ), with 1 second accumulation time for each polarizer setting for state$|\Psi\rangle = |\Psi^-\rangle = \frac{1}{\sqrt{2}}\left(|V\rangle_1|H\rangle_2 - |H\rangle_1|V\rangle_2\right)$. The S value is consistent with equation 4.12 since $2 \leq S = 2.658 \pm 0.006 \leq 2\sqrt{2}$, the violation of CHSH inequality shows the photon source is highly-entangled, refuting the hidden variable theory, which was first experimentally demosntrated by Kwiat at 1995 [22].

Chapter 5

Conclusion and Future outlook

5.1 Conclusion

In conclusion, we bulid a high brightness telecom band entangled photonic source with the Sagnac interferometer as the core part. The single path counts is approximately half-million per second, and the maximum generation rate of entangled photon pairs is $120k/s$, which is 500 times higher than the previous entangled photon source that built by P. G. Evans at 2010 with a GVM-PPKTP crystal at telecom wavelength [23]. The high single path counts and the high entangled photon pair counts indicate the high brightness.

The wavelength of the generated photons is centered at 1550nm telecom band which had been efficiently detected by 1550nm centered superconducting nanowire single-photon detector (SNSPD). Our source also shows an excellent quantum behaviour, with the $|H\rangle$ basis visibility $V_H = 97.7\%$ and the $|+\rangle$ basis visibility $V_+ = 87.2\%$. We measured the Bell parameter S, obtained $S = 2.658 \pm 0.006$, which violates the CHSH inequality by 114 standard deviations. The high visibility and the violation of CHSH inequality demonstrate that the source is highly quantum entangled.

5.2 Future outlook

During the last two decades, quantum mechanism has been well studied experimentally in many experimental settings, includes entangled quantum pair generation, quantum key distribution, quantum dense coding, quantum

teleportation, quantum walk and quantum machine learning based on the photonic systems [24–33].

We can perform the thermal control and the optimization of filter to both increase the brightness and purity of this source. Further more, the effort of building this Sagnac interferometer based source paves the way for compact waveguide-based entanglement source with PPLN crystal which can generate GHZ photon pair rates . The SPDC source also can work as a complementarity of quantum dots for the quantum teleportation between KTH and Kista. Last but not least, this source can help us study the photons behaviour in the topological photonic crystal in the quantum region.

Bibliography

[1] Schrödinger, E. “Discussion of Probability Relations between Separated Systems”. In: *Mathematical Proceedings of the Cambridge Philosophical Society* 31.4 (1935), pp. 555–563. DOI: 10.1017/S0305004100013554.

[2] Bouwmeester, Dik, Pan, Jian-Wei, Mattle, Klaus, Eibl, Manfred, Weinfurter, Harald, and Zeilinger, Anton. “Experimental quantum teleportation”. In: *Nature* 390.6660 (1997), pp. 575–579.

[3] Pan, Jian-Wei, Chen, Zeng-Bing, Lu, Chao-Yang, Weinfurter, Harald, Zeilinger, Anton, and Żukowski, Marek. “Multiphoton entanglement and interferometry”. In: *Reviews of Modern Physics* 84.2 (2012), p. 777.

[4] Kim, Isaac I, McArthur, Bruce, and Korevaar, Eric J. “Comparison of laser beam propagation at 785 nm and 1550 nm in fog and haze for optical wireless communications”. In: *Optical wireless communications III*. Vol. 4214. Spie. 2001, pp. 26–37.

[5] Dirac, Paul Adrien Maurice. *The principles of quantum mechanics*. 27. Oxford university press, 1981.

[6] Gerry, Christopher, Knight, Peter, and Knight, Peter L. *Introductory quantum optics*. Cambridge university press, 2005.

[7] Wootters, W. K. and Zurek, W. H. “A single quantum cannot be cloned”. In: 299.5886 (Oct. 1982), pp. 802–803. DOI: 10.1038/299802a0.

[8] Shalm, Lynden K., Meyer-Scott, Evan, Christensen, Bradley G., Bierhorst, Peter, Wayne, Michael A., Stevens, Martin J., Gerrits, Thomas, Glancy, Scott, Hamel, Deny R., Allman, Michael S., Coakley, Kevin J., Dyer, Shellee D., Hodge, Carson, Lita, Adriana E., Verma, Varun B., Lambrocco, Camilla, Tortorici, Edward, Migdall, Alan L., Zhang, Yanbao, Kumor, Daniel R., Farr, William H., Marsili, Francesco, Shaw, Matthew D., Stern, Jeffrey A., Abellán, Carlos, Amaya,

Waldimar, Pruneri, Valerio, Jennewein, Thomas, Mitchell, Morgan W., Kwiat, Paul G., Bienfang, Joshua C., Mirin, Richard P., Knill, Emanuel, and Nam, Sae Woo. “Strong Loophole-Free Test of Local Realism”. In: *Phys. Rev. Lett.* 115 (25 Dec. 2015), p. 250402. DOI: 10.1103/PhysRevLett.115.250402. URL: https://link.aps.org/doi/10.1103/PhysRevLett.115.250402.

[9] Bell, John S. “On the einstein podolsky rosen paradox”. In: *Physics Physique Fizika* 1.3 (1964), p. 195.

[10] Nielsen, Michael A and Chuang, Isaac. *Quantum computation and quantum information*. 2002.

[11] Harris, S. E., Oshman, M. K., and Byer, R. L. “Observation of Tunable Optical Parametric Fluorescence”. In: *Phys. Rev. Lett.* 18 (18 May 1967), pp. 732–734. DOI: 10.1103/PhysRevLett.18.732. URL: https://link.aps.org/doi/10.1103/PhysRevLett.18.732.

[12] Otero Casal, Pedro. *Spontaneous Parametric Down-Conversion*. 2022.

[13] Armstrong, J. A., Bloembergen, N., Ducuing, J., and Pershan, P. S. “Interactions between Light Waves in a Nonlinear Dielectric”. In: *Phys. Rev.* 127 (6 Sept. 1962), pp. 1918–1939. DOI: 10.1103/PhysRev.127.1918. URL: https://link.aps.org/doi/10.1103/PhysRev.127.1918.

[14] Hum, David S and Fejer, Martin M. “Quasi-phasematching”. In: *Comptes Rendus Physique* 8.2 (2007), pp. 180–198.

[15] Zumsteg, FC, Bierlein, JD, and Gier, TE. “K x Rb1- x TiOPO4: a new nonlinear optical material”. In: *Journal of Applied Physics* 47.11 (1976), pp. 4980–4985.

[16] Fiorentino, Marco, Messin, Gaétan, Kuklewicz, Christopher E., Wong, Franco N. C., and Shapiro, Jeffrey H. “Generation of ultrabright tunable polarization entanglement without spatial, spectral, or temporal constraints”. In: *Phys. Rev. A* 69 (4 Apr. 2004), p. 041801. DOI: 10.1103/PhysRevA.69.041801. URL: https://link.aps.org/doi/10.1103/PhysRevA.69.041801.

[17] Kim, Taehyun, Fiorentino, Marco, and Wong, Franco N. C. “Phase-stable source of polarization-entangled photons using a polarization Sagnac interferometer”. In: *Phys. Rev. A* 73 (1 Jan. 2006), p. 012316. DOI: 10.1103/PhysRevA.73.012316. URL: https://link.aps.org/doi/10.1103/PhysRevA.73.012316.

[18] Esmaeil Zadeh, Iman, Los, Johannes WN, Gourgues, Ronan BM, Steinmetz, Violette, Bulgarini, Gabriele, Dobrovolskiy, Sergiy M, Zwiller, Val, and Dorenbos, Sander N. "Single-photon detectors combining high efficiency, high detection rates, and ultra-high timing resolution". In: *Apl Photonics* 2.11 (2017), p. 111301.

[19] Esmaeil Zadeh, Iman, Chang, J, Los, Johannes WN, Gyger, Samuel, Elshaari, Ali W, Steinhauer, Stephan, Dorenbos, Sander N, and Zwiller, Val. "Superconducting nanowire single-photon detectors: A perspective on evolution, state-of-the-art, future developments, and applications". In: *Applied Physics Letters* 118.19 (2021), p. 190502.

[20] Clauser, John F., Horne, Michael A., Shimony, Abner, and Holt, Richard A. "Proposed Experiment to Test Local Hidden-Variable Theories". In: *Phys. Rev. Lett.* 23 (15 Oct. 1969), pp. 880–884. DOI: 10.1103/PhysRevLett.23.880. URL: https://link.aps.org/doi/10.1103/PhysRevLett.23.880.

[21] Bohm, David. "A Suggested Interpretation of the Quantum Theory in Terms of "Hidden" Variables. I". In: *Physical Review* 85.2 (Jan. 1952), pp. 166–179. DOI: 10.1103/PhysRev.85.166.

[22] Kwiat, Paul G., Mattle, Klaus, Weinfurter, Harald, Zeilinger, Anton, Sergienko, Alexander V., and Shih, Yanhua. "New High-Intensity Source of Polarization-Entangled Photon Pairs". In: *Phys. Rev. Lett.* 75 (24 Dec. 1995), pp. 4337–4341. DOI: 10.1103/PhysRevLett.75.4337. URL: https://link.aps.org/doi/10.1103/PhysRevLett.75.4337.

[23] Evans, P. G., Bennink, R. S., Grice, W. P., Humble, T. S., and Schaake, J. "Bright Source of Spectrally Uncorrelated Polarization-Entangled Photons with Nearly Single-Mode Emission". In: *Phys. Rev. Lett.* 105 (25 Dec. 2010), p. 253601. DOI: 10.1103/PhysRevLett.105.253601. URL: https://link.aps.org/doi/10.1103/PhysRevLett.105.253601.

[24] Pan, Jian-Wei, Bouwmeester, Dik, Weinfurter, Harald, and Zeilinger, Anton. "Experimental Entanglement Swapping: Entangling Photons That Never Interacted". In: *Phys. Rev. Lett.* 80 (18 May 1998), pp. 3891–3894. DOI: 10.1103/PhysRevLett.80.3891. URL: https://link.aps.org/doi/10.1103/PhysRevLett.80.3891.

[25] Bouwmeester, Dik, Pan, Jian-Wei, Daniell, Matthew, Weinfurter, Harald, and Zeilinger, Anton. “Observation of Three-Photon Greenberger-Horne-Zeilinger Entanglement”. In: *Phys. Rev. Lett.* 82 (7 Feb. 1999), pp. 1345–1349. DOI: 10.1103/PhysRevLett.82.1345. URL: https://link.aps.org/doi/10.1103/PhysRevLett.82.1345.

[26] Liao, Sheng-Kai, Cai, Wen-Qi, Liu, Wei-Yue, Zhang, Liang, Li, Yang, Ren, Ji-Gang, Yin, Juan, Shen, Qi, Cao, Yuan, Li, Zheng-Ping, et al. “Satellite-to-ground quantum key distribution”. In: *Nature* 549.7670 (2017), pp. 43–47.

[27] Kitagawa, Takuya, Broome, Matthew A, Fedrizzi, Alessandro, Rudner, Mark S, Berg, Erez, Kassal, Ivan, Aspuru-Guzik, Alán, Demler, Eugene, and White, Andrew G. “Observation of topologically protected bound states in photonic quantum walks”. In: *Nature communications* 3.1 (2012), pp. 1–7.

[28] Gao, Jun, Qiao, Lu-Feng, Jiao, Zhi-Qiang, Ma, Yue-Chi, Hu, Cheng-Qiu, Ren, Ruo-Jing, Yang, Ai-Lin, Tang, Hao, Yung, Man-Hong, and Jin, Xian-Min. “Experimental Machine Learning of Quantum States”. In: *Phys. Rev. Lett.* 120 (24 June 2018), p. 240501. DOI: 10.1103/PhysRevLett.120.240501. URL: https://link.aps.org/doi/10.1103/PhysRevLett.120.240501.

[29] Ji, Ling, Gao, Jun, Yang, Ai-Lin, Feng, Zhen, Lin, Xiao-Feng, Li, Zhong-Gen, and Jin, Xian-Min. “Towards quantum communications in free-space seawater”. In: *Opt. Express* 25.17 (Aug. 2017), pp. 19795–19806. DOI: 10.1364/OE.25.019795. URL: http://opg.optica.org/oe/abstract.cfm?URI=oe-25-17-19795.

[30] Reimer, Michael E, Bulgarini, Gabriele, Akopian, Nika, Hocevar, Moïra, Bavinck, Maaike Bouwes, Verheijen, Marcel A, Bakkers, Erik PAM, Kouwenhoven, Leo P, and Zwiller, Val. “Bright single-photon sources in bottom-up tailored nanowires”. In: *Nature communications* 3.1 (2012), pp. 1–6.

[31] Zhong, Han-Sen, Wang, Hui, Deng, Yu-Hao, Chen, Ming-Cheng, Peng, Li-Chao, Luo, Yi-Han, Qin, Jian, Wu, Dian, Ding, Xing, Hu, Yi, et al. “Quantum computational advantage using photons”. In: *Science* 370.6523 (2020), pp. 1460–1463.

[32] Elshaari, Ali W, Pernice, Wolfram, Srinivasan, Kartik, Benson, Oliver, and Zwiller, Val. “Hybrid integrated quantum photonic circuits”. In: *Nature Photonics* 14.5 (2020), pp. 285–298.

[33] Elshaari, Ali W, Zadeh, Iman Esmaeil, Fognini, Andreas, Reimer, Michael E, Dalacu, Dan, Poole, Philip J, Zwiller, Val, and Jöns, Klaus D. “On-chip single photon filtering and multiplexing in hybrid quantum photonic circuits”. In: *Nature communications* 8.1 (2017), pp. 1–8.